# XIAP Protects Retinal Ganglion Cells in the Mutant ND4 Mouse Model of Leber Hereditary Optic Neuropathy

Sarah J. Wassmer,[1,*] Yves De Repentigny,[2] Derek Sheppard,[3] Pamela S. Lagali,[2] Lijun Fang,[4] Stuart G. Coupland,[1,2,5] Rashmi Kothary,[1,2] John Guy,[6] William W. Hauswirth,[7] and Catherine Tsilfidis[1,2,5]

[1]Department of Cellular and Molecular Medicine, University of Ottawa, Ottawa, Ontario, Canada
[2]Ottawa Hospital Research Institute, Regenerative Medicine, Ottawa, Ontario, Canada
[3]Department of Biology, Carleton University, Ottawa, Ontario, Canada
[4]Department of Ophthalmology, Fujian Medical University Union Hospital, Fuzhou, China
[5]Department of Ophthalmology, University of Ottawa, Ottawa, Ontario, Canada
[6]Bascom Palmer Eye Institute, University of Miami, Miami, Florida, United States
[7]Department of Ophthalmology, University of Florida College of Medicine, Gainesville, Florida, United States

Correspondence: Catherine Tsilfidis, Ottawa Hospital Research Institute, 501 Smyth Road, K1H 8L6 Canada; ctsilfidis@ohri.ca.

*Current affiliation: Centre for Commercialization of Regenerative Medicine, Toronto, Ontario, Canada

**Received:** July 31, 2019
**Accepted:** May 15, 2020
**Published:** July 31, 2020

Citation: Wassmer SJ, De Repentigny Y, Sheppard D, et al. XIAP protects retinal ganglion cells in the mutant ND4 mouse model of leber hereditary optic neuropathy. *Invest Ophthalmol Vis Sci.* 2020;61(8):49. https://doi.org/10.1167/iovs.61.8.49

**Purpose.** Leber hereditary optic neuropathy (LHON) is a genetic form of vision loss that occurs primarily owing to mutations in the nicotinamide adenine dinucleotide dehydrogenase (ND) subunits that make up complex I of the electron transport chain. LHON mutations result in the apoptotic death of retinal ganglion cells. We tested the hypothesis that gene therapy with the X-linked inhibitor of apoptosis (XIAP) would prevent retinal ganglion cell apoptosis and reduce disease progression in a vector-induced mouse model of LHON that carries the ND4 mutation.

**Methods.** Adeno-associated virus (AAV) encoding full length hemagglutinin-tagged XIAP (AAV2.HA-XIAP) or green fluorescent protein (AAV2.GFP) was injected into the vitreous of DBA/1J mice. Two weeks later, the LHON phenotype was induced by AAV delivery of mutant ND4 (AAV2.mND4FLAG) to the vitreous. Retinal function was assessed by pattern electroretinography. Optic nerves were harvested at 4 months, and the effects of XIAP therapy on nerve fiber layer and optic nerve integrity were evaluated using immunohistochemistry, transmission electron microscopy and magnetic resonance imaging.

**Results.** During LHON disease progression, retinal ganglion cell axons are lost. Apoptotic cell bodies are seen in the nuclei of astrocytes or oligodendrocytes in the optic nerve, and there is thinning of the optic nerve and the nerve fiber layer of the retina. At 4 months after disease onset, XIAP gene therapy protects the nerve fiber layer and optic nerve architecture by preserving axon health. XIAP also decreases nuclear fragmentation in resident astrocytes or oligodendrocytes and decreases glial cell infiltration.

**Conclusions.** XIAP therapy improves optic nerve health and delays disease progression in LHON.

Keywords: Leber hereditary optic neuropathy, XIAP, gene therapy

Leber hereditary optic neuropathy (LHON) is a maternally inherited optic neuropathy that is characterized by central vision loss. More than 95% of cases of LHON are caused by mutations within the mitochondrial ND4 (G11778A), ND1 (G3460A), and ND6 (T14484) genes.[1] These three mutations pose a significant risk of developing vision loss owing to retinal ganglion cell (RGC) death, optic disc atrophy, optic nerve myelin pathology (including oligodendrocyte degeneration) and glial cell activation.[2]

Insights into the effects of LHON mutations have been provided by cellular hybrid (cybrid) cell lines generated by introducing LHON mutant mitochondrial DNA into mitochondrial DNA-depleted cells. Studies in these cells have shown defects in mitochondrial function characterized by decreased adenosine triphosphate levels, decreases in mitochondrial inner membrane potential, and increased superoxide levels.[3] How these defects lead to RGC degeneration is unknown; however, a number of studies have suggested that they make RGCs more susceptible to apoptotic cell death. For example, cybrids carrying the ND1 and ND4 mutations are sensitized to Fas-induced apoptosis and can be rescued by incubation with the synthetic caspase inhibitor, zVAD-fmk.[4] LHON mutation-carrying cybrids also undergo apoptotic cell death when grown in galactose rather than glucose medium (which forces the cells to use mitochondrial respiration to generate adenosine triphosphate). The cell death is accompanied by an increase in mitochondrial cytochrome c release into the cytosol.[5] Studies in LHON patient peripheral

blood lymphocytes show increased apoptosis in comparison with healthy controls upon treatment with an oxidizing agent, and this result is attributed to the involvement of the mitochondria in the activation of the apoptotic cascade.[6]

The X-linked Inhibitor of Apoptosis (XIAP) is the most potent inhibitor of apoptosis within the Inhibitor of Apoptosis family of proteins. It binds to and inhibits caspases 3, 7, and 9 and further mediates caspase degradation via the E3 ligase activity of its C-terminal RING domain.[7–9] Furthermore, it has been shown that XIAP can enter the mitochondria to compete with Bax/Bak-mediated mitochondrial outer membrane permeabilization to suppress mitochondrial-mediated cell death.[10,11] Thus, XIAP is able to block both the mitochondrial (intrinsic) and death receptor-mediated (extrinsic) apoptotic cascades. Moreover, XIAP has additional functions that are unrelated to its role in caspase inhibition. XIAP and related family members cIAP1 and cIAP2 can inhibit the "ripoptosome," which is involved in necroptosis.[12–14] In addition, XIAP has been shown to regulate the nuclear factor-$\kappa$B and JNK pathways[15–17] to suppress TNF-$\alpha$– and TGF-$\beta$1–induced apoptosis.[16] More recent studies point to a critical role for XIAP in reducing inflammation and a role in innate immunity.[18,19]

The LHON phenotype has been successfully replicated in DBA/1J mice by adeno-associated viral delivery of mutant nicotinamide adenine dinucleotide dehydrogenase 4 (mND4) to the mitochondria of RGCs.[20–24] Studies in these mice have confirmed that RGC loss is due to apoptosis.[22] Because many visual disorders involve the ultimate death of retinal cells by apoptosis, antiapoptotic therapy holds tremendous promise as a general treatment for multiple types of retinal disease. To date, adeno-associated virus (AAV)-mediated XIAP gene therapy has been used to effectively protect RGCs in rat models of retinal ischemia[25] and glaucoma.[26] XIAP has also been shown to protect photoreceptor structure and function in chemically induced retinal degeneration[27,28] and in retinitis pigmentosa.[29] In animal models of retinal detachment, XIAP preserved photoreceptor structure for up to 2 months of continuous detachment[30] and seemed to preserve photoreceptor function.[31] XIAP also increased the survival of transplanted retinal progenitor cells[32] and prolonged the treatment window in a mouse model of retinal degeneration treated with gene replacement therapy.[33]

Given the success of XIAP gene therapy in multiple forms of retinal degeneration and the fact that RGC loss in LHON is primarily apoptotic in nature, we evaluated the efficacy of XIAP gene therapy in protecting RGCs in a mouse model of LHON. We show that XIAP reduces glial cell infiltration, decreases nuclear fragmentation of resident glial cells in the optic nerve, and preserves RGC axon thickness. XIAP also seems to preserve RGC function.

## Methods

### Adeno-Associated Viral Vectors

AAV2/2 vectors were generated for these studies. All constructs were under the control of the cytomegalovirus immediate early gene enhancer and chicken beta-actin promoter. The AAV2.HA-XIAP vector contained the human XIAP open reading frame with an N-terminal hemagglutinin (HA) tag. Gene expression was enhanced by the presence of a woodchuck postregulatory element in the viral construct. AAV2.GFP virus was similarly generated for use as an injection and viral control. Details of vector construction are found in Renwick et al.[25] Construction of the mutant human R340H ND4 (mND4) construct has been described elsewhere.[22] The mND4 construct (AAV2.mND4FLAG) contained the ATPc mitochondrial targeting sequence to allow the allotopically expressed protein to be shuttled to the mitochondria, and a C-terminal FLAG tag for immunodetection. Triple Y-F AAV vectors were generated and titered as previously described.[34,35] Schematics of each of the viral vectors are found in Supplementary Figure S1.

### Animals and Injection Procedures

Adult male DBA1/J mice were purchased from The Jackson Laboratory and kept under standard 12-hour light/12-hour dark laboratory conditions. All procedures were approved by the University of Ottawa Animal Care and Veterinary Service and adhered to the ARVO statement for the Use of Animals in Ophthalmic and Vision Research. Male mice between the ages of 10 and 12 weeks were used for these studies ($N = 27$). Animals were injected intravitreally in the left eye with 1 µL of $10^{11}$ VG/mL of AAV2.HA-XIAP (i.e., $1 \times 10^8$ total viral particles) and an equal dose of AVV2.GFP in the right eye. Two weeks after the initial injection, one-third of the animals received 1 µL of AAV2.mND4FLAG in the left XIAP-treated eye, one-third received AAV2.mND4FLAG in the right GFP-treated eye, and one-third received AAV2.mND4FLAG in both eyes. AAV2.mND4FLAG was delivered at a dose of $2 \times 10^{12}$ VG/mL (i.e., $2 \times 10^9$ total viral particles). Eyes and optic nerves were sampled at 3 or 4 months after mND4 injection.

### Immunohistochemistry

Enucleated eyes were processed for cryosectioning or flat mounts. Tissue sampling for cryosections was conducted as previously described.[25] For flat mounts, retinas were carefully dissected and flattened onto nitrocellulose membranes with the RGC layer facing upwards. Retinas were fixed for 30 minutes with 4% paraformaldehyde at room temperature and then transferred to PBS at 4°C (for up to 3 days). The retinas were then carefully teased off the membranes and treated with ascending concentrations of sucrose (10%, 20%, and 30%) each for 10 minutes, followed by 3 freeze/thaw cycles on dry ice and room temperature, respectively. The retina flat mounts were mounted onto Superfrost slides (Fisher Scientific, Waltham, MA) in 30% sucrose and placed at –80°C until staining. Hematoxylin and eosin staining was performed according to standard protocols. Immunostaining was performed with anti-FLAG M2-cy3 (1:100, Sigma, St. Louis, MO), anti-HA high affinity (1:100, Sigma), anti-RNA binding protein with multiple splicing (RBPMS; 1:100, Phosphosolutions, Aurora, CO) and anti-GFP (1:200, Invitrogen, Carlsbad, CA). All primary antibodies were incubated for 2 days. Secondary antibodies conjugated to Alexa 488 (Invitrogen) and Cy3 (Jackson ImmunoResearch, West Grove, PA) fluorophores were used at 1:500 and incubated at room temperature for 1 hour.

### Western Blot

Twenty micrograms of protein was separated by electrophoresis on 12% polyacrylamide gels, and transferred onto PVDF membranes. Membranes were blocked for 1

Investigative Ophthalmology & Visual Science

hour at 4°C in 5% powdered milk, and incubated overnight at 4°C with primary rabbit anti-GST-XIAP (1:5000 in blocking buffer; courtesy of Dr. Robert Korneluk, University of Ottawa) or rabbit anti-Bim (1:1000, Cell Signaling Technology, Danvers, MA). Membranes were washed and incubated for one hour at room temperature in anti-rabbit horseradish peroxidase or anti-rabbit IRDye 800 (Li-Cor, Lincoln, NE). Proteins were visualized using Pierce Chemiluminescence substrates (ThermoFisher Scientific, Waltham, MA) and film, or the Licor imaging system.

### Preparation of Optic Nerves for Transmission Electron Microscopy

DBA/1J mice were anesthetized by intraperitoneal injection of tribromoethanol (Avertin). Perfusions and tissue processing, embedding and sectioning were conducted as previously described.[36] Ultrathin sections (80 nm) were observed under a transmission electron microscope (Hitachi 7100) at 2000×, 4000×, 10,000×, and 20,000× magnifications. Ultrastructural analysis was conducted on approximately 300 electron micrographs of left and right optic nerves at the central region of the optic nerve.

### Toluidine Blue Staining for Electron Microscopy Semithin Sections

Semithin cross-sections of 0.5 µm from resin embedded central segment of optic nerves were mounted on glass slides and stained with 1% toluidine blue and 2% borate in distilled water. Sections were scanned with a MIRAX MIDI (Zeiss, Jena, Germany) and observed at 60× and 400× magnifications using a Zeiss MIRAX Viewer software. Stained sections were also examined by light microscopy using a Zeiss Axioplan microscope equipped with a digital camera for a quantitative analysis of myelinated axons.

### Axon Counts

Toluidine blue images containing scale bars were imported into ImageJ and processed using the Enhance Local Contrast Plugin. After the scale bar was set, two grids of 1300 µm$^2$ were overlaid on the image and axons were counted using the Cell Counter Plugin at 150% zoom. An average of five images (10 grids) was counted for each optic nerve and the numbers averaged to get a mean count per grid for each optic nerve. The grids were placed in the center, top, bottom, left, and right quadrants of every nerve so that there was no bias in selecting the areas to be counted.

To determine cross-sectional areas of axons, images imported into ImageJ were scaled and processed using the contrast limited adaptive histogram equalization (CLAHE) plugin. Using the Threshold Colour Plugin, "threshold" and "invert" were selected, and the brightness was adjusted to allow visualization of the axons. The image was converted to 8-bit and the threshold color was adjusted to red. Axonal cross-sectional areas were determined using the Analyze Particles Plugin with size set to "0–infinity" and circularity set to "0.3–1.0". The number and proportion of axons with a cross-sectional area of less than 1 µm$^2$ was recorded.

### Pattern ERG (PERG)

PERGs were recorded on the Espion E$^2$ system (Diagnosys, Inc., Lowell, MA). The mice were anesthetized with ketamine (50 mg/kg) and medetomidine (1 mg/kg) and placed on an elevated heated (37°C) platform 20 cm from a computer monitor. The monitor displayed 200 mm interspaced black and white bars at 50 cd/m$^2$, 0.05 cycles/deg, 100% contrast, and 2 Hz temporal frequency. A 2-mm diameter gold loop electrode was placed on the undilated pupil facing the screen. A total of 1800 traces were recorded (two consecutive sequences of 900 traces, sample frequency 1000 Hz, sweep duration of 10 ms before stimulus to 400 ms after stimulus). Retinal signals were amplified (10,000 fold) and a band-pass filter of 0.3 to 300.0 Hz was used. The reference stainless steel needle electrode was placed in the scalp and the ground electrode was placed in the tail. Final waveforms were scored by removing all outlier traces above +30 µV and below −30 µV.

### Magnetic Resonance Imaging

A 7T GE/Agilent MR 901 magnetic resonance imaging machine was used to generate cross-sectional images of eight orbits (three mice with right eye injected with AAV2.HAXIAP and AAV2.mND4FLAG, and left eye injected with AAV2.GFP and AAV2.mND4FLAG, and seven uninjected controls). Animals were anesthetized for the magnetic resonance imaging procedure with isoflurane. Each orbit was imaged with a fast spin echo pulse sequence, with an echo time of 25 ms, repetition time of 1075 ms, slice thickness of 350 µm, and in-plane spatial resolution of 78 µm. The slices were oriented in an oblique fashion so that the entire length of the optic nerve would lie completely within the plane of one of the slices. Images were imported into ImageJ[37] and optic nerve diameters were measured at the same distance from the optic disc in each image. Measurements were taken by three independent observers who were blind to the experimental groups. All observers obtained similar results. The values generated by one independent observer are reported.

### Viability Assays

The transformed cone photoreceptor cell line, 661W, was kindly provided by Dr. M. Al-Ubaiddi.[38] The 661W cells were transfected with the full-length coding sequence of human XIAP, which was generated from pCM-SPORT6-XIAP (Origene, Rockville, MD) digested with SalI and NotI to isolate the XIAP coding sequence, ligated into the pCI-neo vector (Promega, Madison, WI). Transfections were conducted using Lipofectamine 2000 (ThermoFisher Scientific), according to the manufacturer's instructions. Control cell lines were transfected in a similar manner with the pCI-neo empty vector. Stably expressing cells were grown under G418 selection. All cells were used below passage 15, and XIAP expression was monitored in each assay by Western blot or quantitative RT-PCR.

For the death assays, cells were plated onto 96-well plates at 60% confluency and incubated with 1 mM hydrogen peroxide (Sigma Aldrich) for 32 hours or 15 µM menadione (Sigma Aldrich) for 4 hours. Cell viability was measured using the AlamarBlue Cell Viability Reagent (Invitrogen) and a Synergy BioTek plate reader (BioTek Instruments, Inc.) as per manufacturer's directions. Read-out measurements of

Investigative Ophthalmology & Visual Science

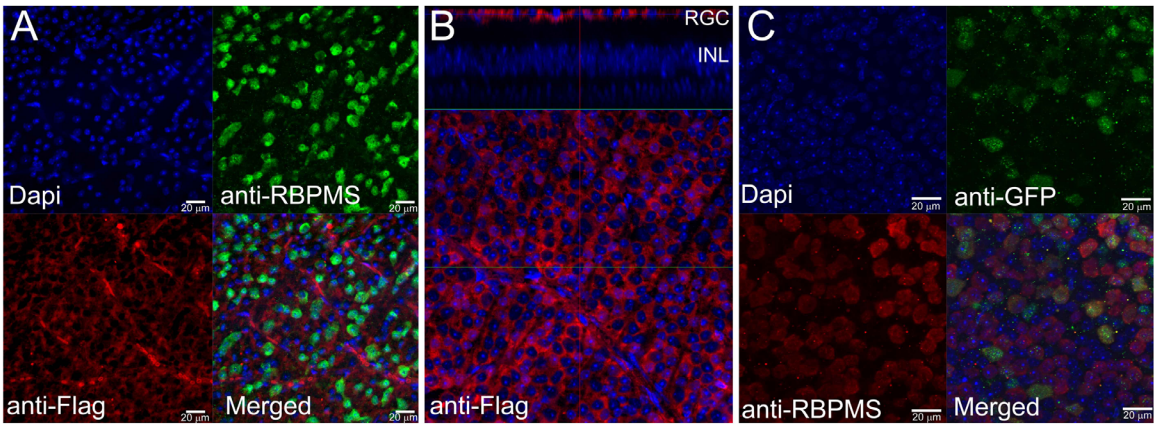


**Figure 1.** mND4 and GFP expression in the retina after AAV2 intravitreal injection. (**A**) Immunofluorescent images of a retinal flat mount of an eye injected with AAV2.mND4FLAG and stained with the nuclear marker DAPI (*blue*), anti-RNA binding protein with multiple splicing (RBPMS) antibody to identify RGCs (*green*) and an antibody to the FLAG tag to show the localization of the mND4 protein. There is robust perinuclear mND4 expression. (**B**) Perinuclear staining for mND4 is confirmed in a second retinal flat mount. Z-stack confocal microscopy shows that the mND4 (FLAG-tag) is present in the RGC layer of the retina. (**C**) Immunofluorescent images of a retinal flat mount of an AAV2.GFP-injected retina show co-localization of GFP (*green*) and RGC marker RBPMS (*red*).

treated cells were divided by vehicle control-treated cells to determine final viability. Three individual plates with five replicates each were averaged.

## Results

### XIAP Overexpression Protects Against Oxidative Stress-Induced Photoreceptor Cell Death In Vitro

Oxidative stress is a major factor in the ultimate death of RGCs in LHON. The ability of XIAP to protect against oxidative stress-induced apoptosis in retinal cells in vitro was shown in a previous study from our lab[31] and confirmed with additional XIAP over-expressing cell lines for the current study (Supplementary Fig. S2). XIAP was able to significantly protect 661W photoreceptor cells from menadione- and hydrogen peroxide-induced cell death (Supplementary Fig. S2B–C). One potential mechanism through which XIAP may be mediating cellular protection is by the downregulation of the proapoptotic protein Bim (Supplementary Fig. S3).

### Mutant ND4 Induces RGC Axon Thinning

A preliminary 3-month experiment was conducted to examine the disease timeline and to inform the subsequent gene therapy studies. For these studies, AAV2/2 vectors expressing mND4 with an *N*-terminal mitochondrial targeting sequence and a C-terminal FLAG tag (AAV2.mND4FLAG) were delivered into the vitreous of the mouse eye. AAV2.GFP was injected in the contralateral eye as a control. Because ND4 is a mitochondrial gene, the mitochondrial targeting sequence ensured that the allotopically expressed protein product would be directed to the mitochondria. Three months after the injection, retinal flat mounts ($n = 10$) were used to assess the presence of the virally expressed proteins in RGCs (Fig. 1). There was strong mND4 expression throughout the inner retina that was mostly restricted to the RGC layer and showed a widespread perinuclear pattern within RGCs (that were co-labeled with the RGC marker RNA binding protein with multiple splicing) (Figs. 1A–B). Contralateral GFP-injected retinas showed infection of most cells in the RGC layer, although the level of expression of GFP was variable between cells (Fig. 1C).

An analysis of sampled tissues showed degenerative changes in the mND4-injected optic nerves (Supplementary Fig. S4), decreased axon counts (Supplementary Fig. S5), and nerve fiber layer thinning (Supplementary Fig. S6), confirming that the mND4 construct was able to replicate characteristics of human LHON pathology. However, the disease characteristics seen at three months after mND4 delivery to the retina were variable, with some animals clearly showing significant signs of axon loss, and others showing few changes (Supplementary Fig. S5). This finding indicates that the 3-month timepoint represents an early stage of the disease when pathological changes are emerging but not fully established in all animals; consequently, we conducted a more extended (4-month) disease time course for the subsequent study, which examined the ability of XIAP to protect RGCs from LHON disease progression.

### XIAP Gene Therapy in the Mouse Model of LHON

For the gene therapy studies, animals received an intravitreal injection of the *N*-terminus HA-tagged XIAP (AAV2.HA-XIAP) in one eye and AAV2.GFP in the contralateral eye. Two weeks later, the animals received AAV2.mND4FLAG in the XIAP-treated eye, in the GFP-treated eye or in both eyes. The dose of the mND4 virus was increased from $1 \times 10^8$ total viral particles/eye (in the initial study described above) to $2 \times 10^9$ total viral particles per eye to accelerate disease progression. In vivo fundus imaging 2 weeks after the second set of injections showed GFP fluorescence (Fig. 2A), which was confirmed by immunolabeling in AAV2.GFP/ AAV2.mND4FLAG double-injected retinas. Immunolabeling with HA and FLAG antibodies (representing XIAP and mND4, respectively) confirmed that all viral constructs were functional, and showed the continued presence of the proteins in the RGC layer 4 months after AAV2.mND4FLAG injection (Figs. 2B, C and Supplementary Fig. S7).

Investigative Ophthalmology & Visual Science

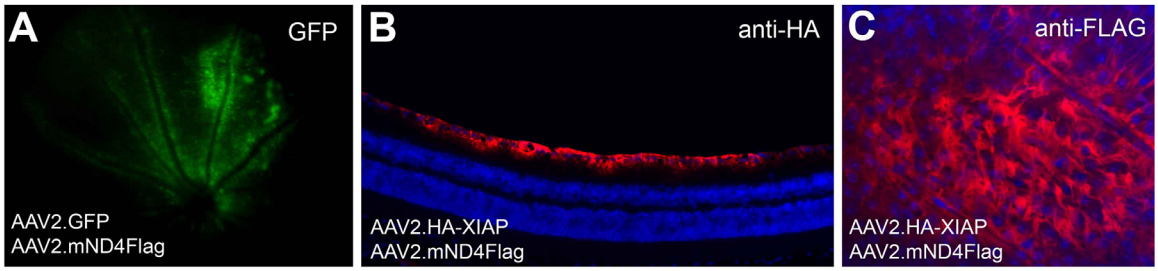


**Figure 2.** Imaging in double-injected retinas confirms expression. (**A**) Fluorescent fundus image of an eye that received both AAV2.GFP and AAV2.mND4FLAG shows GFP expression at two weeks following the second injection, indicating good coverage of the superior retina from the viral injection. (**B**) Immunofluorescent image of a retinal section through an eye that received AAV2.HA-XIAP and AAV2.mND4FLAG. The HA tag shows XIAP expression in the RGC layer. (**C**) Retinal flat mount of an eye that received AAV2.HA-XIAP and then AAV2.mND4FLAG two weeks later shows pockets of mND4 expression in the RGC layer.

### XIAP Overexpression Protects Axon Structure and Function in Early-Onset LHON Disease

The effects of XIAP gene therapy on RGC axon health were analyzed using several parameters. Transmission electron microscopy was conducted in two randomly selected mice that were injected with GFP/mND4 in the right eye and XIAP/mND4 in the left eye. In both animals, the XIAP-treated mND4 eyes showed decreased pathology compared with the GFP-treated mND4 eyes (Fig. 3 and Supplementary Fig. S8), with the differences more pronounced in one animal than the other.

In vivo magnetic resonance imagining was conducted to assess changes in the appearance or thickness of the optic nerve. Optic nerve diameter measurements showed that XIAP-treated optic nerves were significantly thicker (by 14.9%; $P < 0.05$) than their GFP-treated counterparts and were not significantly different from un-injected optic nerves, whereas GFP/mND4 optic nerves were significantly thinner than uninjected controls (Figs. 4A–C).

Axon counts were conducted on cross-sectioned, toluidine blue–stained optic nerves. GFP/mND4-treated eyes showed a 28.5% decrease in axon numbers in comparison with the XIAP/mND4 group (Fig. 4D), but this did not reach significance ($P = 0.06$) based on the high degree of variability between animals. However, cross-sections of optic nerves clearly demonstrated that the mND4 mutation caused axon thinning, indicating that axons were in the process of dying. Measurements of axonal cross-sectional areas revealed that GFP/mND4 animals had significantly higher numbers of thinner axons (51.9% more) in comparison with the XIAP/mND4 animals ($P = 0.05$; Fig. 4E and Supplementary Figs. S9A–B). In support of these data, hematoxylin and eosin staining of retinal cross-sections showed thinning of the nerve fiber layer in GFP/mND4 animals and the preservation of the nerve fiber layer in the majority of XIAP/mND4 animals (Supplementary Fig. S9).

PERGs, which measure RGC function, were recorded to determine whether XIAP gene therapy could preserve RGC function. Although there was variability between animals, PERG analysis at the 3-month timepoint showed that XIAP/mND4 animals had more typical PERG waveforms and stronger N2 amplitudes compared with GFP/mND4 animals (Fig. 5; Supplementary Fig. S10: $P = 0.037$ with one-tailed $t$-test, $P = 0.07$ with 2-tailed $t$-test; $n = 5$).

Overall, in both the initial characterization of the disease and in the subsequent gene therapy studies, mND4 led to optic nerve axon changes, glial cell infiltration, nuclear fragmentation in resident astrocytes or oligodendrocytes, nerve fiber layer thinning, and RGC functional deficits. These degenerative changes were present in the early stages of LHON disease in most of the animals and had not yet resulted in significant losses in axon numbers. XIAP gene therapy significantly decreased axon thinning, preserved optic nerve diameter, decreased retinal nerve fiber layer thinning in the retina, and had a positive impact on retinal function.

## Discussion

LHON symptoms typically present in patients during early adulthood, although the age of onset can vary from childhood to late adulthood.[39] LHON manifests as a bilateral loss of central vision, but often vision loss occurs initially in one eye followed within weeks to months by the contralateral eye.[39] In some cases, the central vision loss may spontaneously improve,[40] but most patients experience gradual deterioration, leading to permanent vision loss. Overall, the human form of the disease presents as a spectrum with differences even between affected individuals carrying the same mutation. We also saw variation in disease progression in the mND4 mouse model of LHON. Some animals presented with severe degeneration of the optic nerve, characterized by severe axon loss, glial cell infiltration, the absence of myelin and large sections of empty spaces in the optic nerve, which was detected as early as 3 months after injection. Conversely, other animals showed modest axon loss and myelin thinning at the later time point of 4 months. A more extended timeline for our studies would likely decrease the variability seen between experimental animals. Other studies using this animal model have examined disease progression at 6 months and 1 year, clearly showing the progressive nature of the disease and the reduced variability in symptoms with an advanced disease timeline.[21,22,24]

The variation in human and mouse disease cannot be attributed to similar mechanisms. Whereas the human disease has potential genetic modifiers[41–43] and clear environmental agonists (such as alcohol and tobacco),[44] the same cannot be said of an inbred, environmentally controlled mouse colony. In the mouse model, the likely sources of variation between animals were the variability of the injection procedure (which may target different numbers of RGCs every time) and the difficulty in targeting the potentially hundreds or thousands of mitochondria within a cell with a mND4 protein that is allotopically

Investigative Ophthalmology & Visual Science

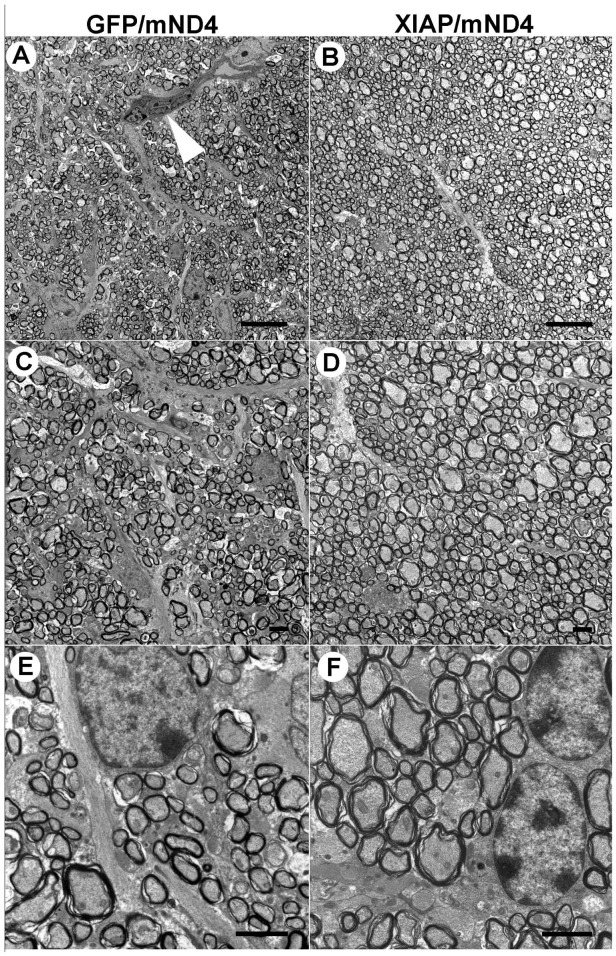


**Figure 3.** Transmission Electron Microscopy (TEM) shows improved optic nerve morphology in XIAP-treated retinas. GFP/mND4 treated eyes (**A**, **C**, **E**) show axonal compaction and thinner cross-sectional areas as well as increased glial cell infiltration and increased nuclear fragmentation of resident glial cells (*white arrowhead* in **A**). By comparison, XIAP/mND4 injected retinas (**B**, **D**, **F**) have thicker axons, less glial cell infiltration and healthier nuclei. Each successive image shows increased magnification of the same optic nerve. Scale bars: **A**, **B** = 10 µm; **C**–**E** = 2 µm.

generated and imported into the mitochondria. In addition, we cannot discount the potential contribution of AAV vector-neutralizing antibodies. Experimental animals received two intravitreal AAV injections: AAV-XIAP or AAV-GFP, followed by AAV-mND4 2 weeks later. The generation of neutralizing antibodies to the AAV vector after the first injection likely decreased the efficacy of the subsequent AAV-mND4 injection.[45] To partly mitigate this effect, we increased the viral dose for the second intravitreal injection from $1 \times 10^8$ to $2 \times 10^9$ total viral particles. Even so, we cannot discount the presence of neutralizing antibodies that added to the variability and modest degeneration in the model. However, we do not believe that the presence of neutralizing antibodies negates the efficacy of the second injection. Yao et al.[46] similarly used intravitreal AAV injections that were 2 weeks apart and showed that both injections led to expression of the transgenes. In our study, we saw a decrease in the expression of the FLAG-tagged ND4 in the double-injected animals in comparison with ones that had received a single AAV injection in the preliminary experiment. Nevertheless, if neutralizing antibodies affected disease variability or progression, the effect would have impacted both GFP- and XIAP-treated eyes equally and, thus, does not alter the significance of the outcomes observed. Interestingly, Li et al.[47] found that the presence of neutralizing antibodies peaks at 2 months after an intravitreal injection. Even though our injections were only two weeks apart (suggesting that the animals did not have maximal levels of circulating AAV2 antibodies), future experiments should deliver dual AAV injections that are less than 3 days apart to eliminate the problem of neutralizing antibodies entirely. In addition, transgenic models of LHON, which have been developed[48,49] and do not require AAV-mediated mND4, may help to decrease some of this variability in future studies.

XIAP efficacy in delaying or preventing retinal cell death was examined both in vitro and in vivo. Owing to a lack of an available RGC cell line, 661W photoreceptor cells were used as a surrogate retinal cell line. Although not predictive of how XIAP would protect RGCs, the 661W studies provided proof of principle for XIAP's efficacy in protecting against oxidative stress and suggested that XIAP may be acting through the downregulation of the proapoptotic protein Bim. Interestingly, studies from the cancer literature suggest that XIAP overexpression can also suppress ROS accumulation in a caspase-independent manner by increasing the expression of antioxidant enzymes SOD1 and SOD2 and that this is dependent on nuclear factor-$\kappa$B activation.[50] Thus, by impacting both caspase-dependent and independent survival pathways, XIAP may be promoting RGC survival through various mechanisms.

The in vivo studies in the LHON model confirmed that XIAP had a significant effect on optic nerve diameter and it significantly reduced the number of thinned axons, maintaining axonal cross-sections at control values. XIAP-treated retinas also had a preserved nerve fiber layer, and optic nerves showed decreased glial cell infiltration and normal myelination. PERGs suggested that XIAP was also able to preserve RGC function. We believe that these XIAP-associated decreases in disease severity during the early stages of the disease examined here would translate into significant protection of RGCs and their axons in later stages of the disease, during which there is significant death of these cells.[24] Notably, we delivered XIAP before inducing LHON to ensure that there would be adequate levels of XIAP expressed in the retina before LHON-associated damage had begun. It would be interesting to evaluate XIAP neuroprotection at later, and therefore, more severe stages of the disease (6 months to 1 year), and to determine if XIAP can protect RGCs from dying after the onset of disease has begun. These studies should, ideally, be conducted in LHON constitutively transgenic animals so that only a single therapeutic injection of AAV2 would be required, thus eliminating the complication of neutralizing antibodies.

The current studies provide proof of principle for XIAP efficacy in the prevention of RGC damage, but treatment before the onset of disease symptoms might not be advisable in human patients. However, given that the disease often manifests in one eye weeks or months before beginning in the second eye, XIAP delivery to the second eye before the advent of symptoms is possible and may prevent severe bilateral disease.

Recently, studies have shown significant rescue and a good safety profile in mouse and nonhuman primate models of LHON treated with AAV2 carrying wildtype ND4.[21,51] The success of these studies has resulted in human clinical

Investigative Ophthalmology & Visual Science

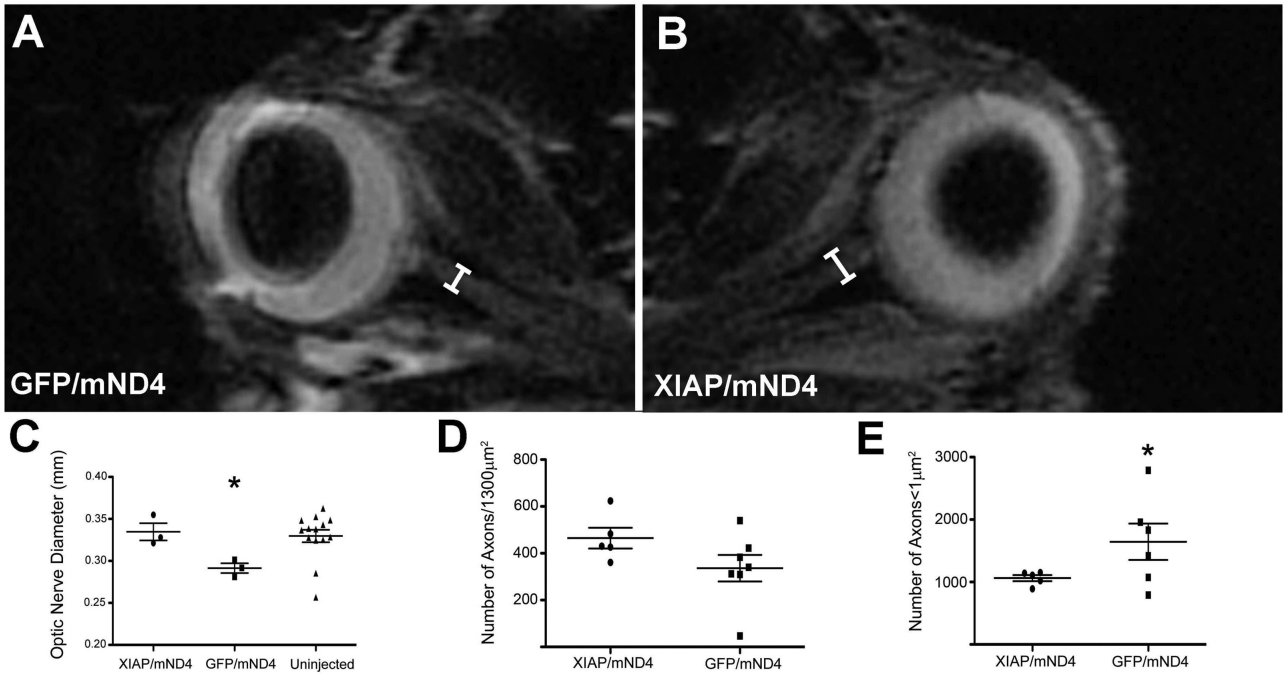


**Figure 4.** Optic nerve measurements show efficacy of XIAP therapy in preserving axonal integrity. (**A**, **B**) Magnetic resonance imaging of the orbit allows measurements of the diameter (*white bar*) of the optic nerve. Measurements were taken at the same distance from the optic cup in all the animals. (**C**) Optic nerve diameters of GFP/mND4-treated retinas are significantly smaller than XIAP/mND4-treated retinas ($P < 0.05$). XIAP-treated optic nerve diameters are similar to un-injected controls. $n = 3$ for XIAP and GFP, $n = 14$ for uninjected controls. (**D**) GFP/mND4-treated eyes show a 28.5% reduction in axon numbers in comparison with the XIAP/mND4 group, but this number does not reach significance ($P = 0.06$) based on the high degree of variability between animals. XIAP $n = 5$, GFP $n = 7$. (**E**) Although there are no significant losses in the number of axons, cross-sections of optic nerves show that the mND4 mutation causes significant axon thinning. There is a significant increase in the number of axons with a cross-sectional area of less than 1 $\mu m^2$ in GFP/mND4-treated retinas in comparison with XIAP/mND4-treated retinas ($P < 0.05$). XIAP $n = 5$, GFP $n = 6$.

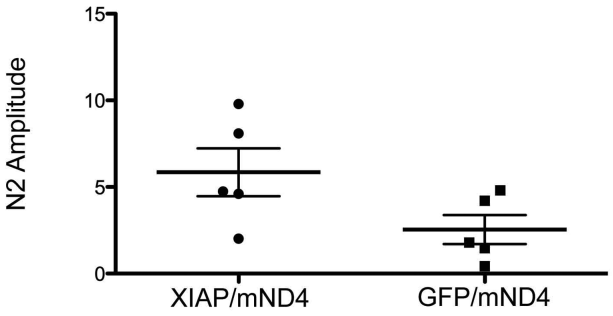


**Figure 5.** PERGs show higher average amplitudes in XIAP/mND4-treated retinas compared with GFP/mND4-treated retinas. Owing to the variability in the disease phenotype caused by insufficient progression of the disease and the small number of animals tested ($n = 5$), the PERG results show a trend towards improved function in XIAP-treated retinas but the results did not reach significance using a two-tailed Student *t*-test ($P = 0.07$); however, given our previous results with XIAP gene therapy and our expectation that XIAP treatment will lead to improved outcomes, a one-tailed Student *t*-test is justifiable, and this leads to a significant result ($P = 0.037$).

trials that are currently underway.[52–56] It remains to be seen whether this therapy will have long-term effects in protecting RGCs, or if the retina will continue to degenerate, similar to the clinical trials (and now marketed therapy) in Leber congenital amaurosis, which showed functional improvements following gene replacement therapy, but continuing retinal degeneration.[57] Based on the promising results obtained in this study, XIAP therapy presents an additional strategy for the treatment of LHON. Moreover, if degeneration continues in the LHON patients in the ongoing clinical trials despite gene replacement, or the results obtained are not optimal, then combination therapy with wild-type ND4 and XIAP may provide a better outcome than either therapy alone. This is supported by a study that used XIAP as an adjunct to AAV-mediated PDE$\beta$ gene replacement therapy in the rd10 mouse and showed that it decreased rates of retinal degeneration compared with AAV-PDE$\beta$ alone.[33] Whether XIAP is delivered alone or as part of a combination therapy, its ability to prevent cell death by targeting apoptosis, reactive oxygen species suppression, necroptosis, and inflammation means that XIAP therapy should be effective in the treatment of a variety of optic neuropathies, irrespective of the type of disease-causing trigger.

## *Acknowledgments*

The authors thank Gregory Cron and his team for performing magnetic resonance imaging. Special thanks are extended to Adam Baker for technical assistance with intravitreal injections and John Hamilton for assistance with pattern electroretinography.

Supported by Canadian Institutes of Health Research (CIHR) and Foundation Fighting Blindness (FFB) grants to CT, CIHR grants to RK, and NIH grant P30-EY021721, MVRF and RPB Inc

funding to WWH. CT is supported by the Don and Joy Maclaren Chair for Vision Research. SW was supported by the David S. Shillito Scholarship in Ophthalmology and by an Ontario Graduate Scholarship.

Disclosure: **S.J. Wassmer,** None; **Y. De Repentigny,** None; **D. Sheppard,** None; **P.S. Lagali,** None; **L. Fang,** None; **S.G. Coupland,** None; **R. Kothary,** None; **J. Guy,** None; **W.W. Hauswirth,** None; **C. Tsilfidis,** None

## *References*

1. Al-Enezi M, Al-Saleh H, Nasser M. Mitochondrial disorders with significant ophthalmic manifestations. *Middle East Afr J Ophthalmol*. 2008;15:81–86.
2. Carelli V, Ross-Cisneros FN, Sadun AA. Optic nerve degeneration and mitochondrial dysfunction: genetic and acquired optic neuropathies. *Neurochem Int*. 2002;40:573–584.
3. Cruz-Bermudez A, Vicente-Blanco RJ, Hernandez-Sierra R, et al. Functional characterization of three concomitant MtDNA LHON mutations shows no synergistic effect on mitochondrial activity. *PLoS One*. 2016;11:e0146816.
4. Danielson SR, Wong A, Carelli V, Martinuzzi A, Schapira AH, Cortopassi GA. Cells bearing mutations causing Leber's hereditary optic neuropathy are sensitized to Fas-Induced apoptosis. *J Biol Chem*. 2002;277:5810–5815.
5. Ghelli A, Zanna C, Porcelli AM, et al. Leber's hereditary optic neuropathy (LHON) pathogenic mutations induce mitochondrial-dependent apoptotic death in transmitochondrial cells incubated with galactose medium. *J Biol Chem*. 2003;278:4145–4150.
6. Battisti C, Formichi P, Cardaioli E, et al. Cell response to oxidative stress induced apoptosis in patients with Leber's hereditary optic neuropathy. *J Neurol Neurosurg Psychiatry*. 2004;75:1731–1736.
7. Berthelet J, Dubrez L. Regulation of apoptosis by inhibitors of apoptosis (IAPs). *Cells*. 2013;2:163–187.
8. Silke J, Vucic D. IAP family of cell death and signaling regulators. *Methods Enzymol*. 2014;545:35–65.
9. Takahashi R, Deveraux Q, Tamm I, et al. A single BIR domain of XIAP sufficient for inhibiting caspases. *J Biol Chem*. 1998;273:7787–7790.
10. Chaudhary AK, Yadav N, Bhat TA, O'Malley J, Kumar S, Chandra D. A potential role of X-linked inhibitor of apoptosis protein in mitochondrial membrane permeabilization and its implication in cancer therapy. *Drug Discov Today*. 2016;21:38–47.
11. Hamacher-Brady A, Brady NR. Bax/Bak-dependent, Drp1-independent targeting of X-linked inhibitor of apoptosis protein (XIAP) into inner mitochondrial compartments counteracts Smac/DIABLO-dependent effector caspase activation. *J Biol Chem*. 2015;290:22005–22018.
12. Vince JE, Wong WW, Gentle I, et al. Inhibitor of apoptosis proteins limit RIP3 kinase-dependent interleukin-1 activation. *Immunity*. 2012;36:215–227.
13. Yabal M, Jost PJ. XIAP as a regulator of inflammatory cell death: the TNF and RIP3 angle. *Mol Cell Oncol*. 2015;2:e964622.
14. Yabal M, Muller N, Adler H, et al. XIAP restricts TNF- and RIP3-dependent cell death and inflammasome activation. *Cell Rep*. 2014;7:1796–1808.
15. Hofer-Warbinek R, Schmid JA, Stehlik C, Binder BR, Lipp J, de Martin R. Activation of NF-kappa B by XIAP, the X chromosome-linked inhibitor of apoptosis, in endothelial cells involves TAK1. *J Biol Chem*. 2000;275:22064–22068.
16. Kaur S, Wang F, Venkatraman M, Arsura M. X-linked inhibitor of apoptosis (XIAP) inhibits c-Jun N-terminal kinase 1 (JNK1) activation by transforming growth factor beta1 (TGF-beta1) through ubiquitin-mediated proteosomal degradation of the TGF-beta1-activated kinase 1 (TAK1). *J Biol Chem*. 2005;280:38599–38608.
17. Lu M, Lin SC, Huang Y, et al. XIAP induces NF-kappaB activation via the BIR1/TAB1 interaction and BIR1 dimerization. *Mol Cell*. 2007;26:689–702.
18. Lawlor KE, Khan N, Mildenhall A, et al. RIPK3 promotes cell death and NLRP3 inflammasome activation in the absence of MLKL. *Nat Commun*. 2015;6:6282.
19. Lawlor KE, Feltham R, Yabal M, et al. XIAP loss triggers RIPK3- and caspase-8-driven IL-1beta activation and cell death as a consequence of TLR-MyD88-induced cIAP1-TRAF2 degradation. *Cell Rep*. 2017;20:668–682.
20. Guy J, Qi X, Koilkonda RD, et al. Efficiency and safety of AAV-mediated gene delivery of the human ND4 complex I subunit in the mouse visual system. *Invest Ophthalmol Vis Sci*. 2009;50:4205–4214.
21. Koilkonda R, Yu H, Talla V, et al. LHON gene therapy vector prevents visual loss and optic neuropathy induced by G11778A mutant mitochondrial DNA: biodistribution and toxicology profile. *Invest Ophthalmol Vis Sci*. 2014;55:7739–7753.
22. Qi X, Sun L, Lewin AS, Hauswirth WW, Guy J. The mutant human ND4 subunit of complex I induces optic neuropathy in the mouse. *Invest Ophthalmol Vis Sci*. 2007;48:1–10.
23. Yu H, Koilkonda RD, Chou TH, et al. Gene delivery to mitochondria by targeting modified adenoassociated virus suppresses Leber's hereditary optic neuropathy in a mouse model. *Proc Natl Acad Sci USA*. 2012;109:E1238–1247.
24. Yu H, Ozdemir SS, Koilkonda RD, et al. Mutant NADH dehydrogenase subunit 4 gene delivery to mitochondria by targeting sequence-modified adeno-associated virus induces visual loss and optic atrophy in mice. *Mol Vis*. 2012;18:1668–1683.
25. Renwick J, Narang MA, Coupland SG, et al. XIAP-mediated neuroprotection in retinal ischemia *Gene Ther*. 2006;13:339–347.
26. McKinnon SJ, Lehman DM, Tahzib NG, et al. Baculoviral IAP repeat-containing-4 protects optic nerve axons in a rat glaucoma model. *Mol Ther*. 2002;5:780–787.
27. Petrin D, Baker A, Brousseau J, et al. XIAP protects photoreceptors from N-methyl-N-nitrosourea-induced retinal degeneration. In: LaVail MM, Hollyfield JG, Anderson RE (Eds), *Retinal degenerations: mechanisms and experimental therapy*. New York: Kluwer Academic/Plenum Publishers; 2003:385–393.
28. Petrin D, Baker A, Coupland SG, et al. Structural and functional protection of photoreceptors from MNU-induced retinal degeneration by the X-linked inhibitor of apoptosis. *Invest Ophthalmol Vis Sci*. 2003;44:2757–2763.
29. Leonard KC, Petrin D, Coupland SG, et al. XIAP protection of photoreceptors in animal models of retinitis pigmentosa. *PLoS ONE*. 2007;2:e314.
30. Zadro-Lamoureux LA, Zacks DN, Baker AN, Zheng QD, Hauswirth WW, Tsilfidis C. XIAP effects on retinal detachment-induced photoreceptor apoptosis [corrected]. *Invest Ophthalmol Vis Sci*. 2009;50:1448–1453.
31. Wassmer SJ, Leonard BC, Coupland SG, et al. Overexpression of the X-Linked inhibitor of apoptosis protects against retinal degeneration in a feline model of retinal detachment. *Hum Gene Ther*. 2017;28:482–492.
32. Yao J, Feathers KL, Khanna H, et al. XIAP therapy increases survival of transplanted rod precursors in a degenerating host retina. *Invest Ophthalmol Vis Sci*. 2011;52:1567–1572.
33. Yao J, Jia L, Khan N, et al. Caspase inhibition with XIAP as an adjunct to AAV vector gene-replacement therapy: improving

efficacy and prolonging the treatment window. *PLoS One*. 2012;7:e37197.

34. Hauswirth WW, Lewin AS, Zolotukhin S, Muzyczka N. Production and purification of recombinant adeno-associated virus. *Methods Enzymol*. 2000;316:743–761.
35. Zolotukhin S, Potter M, Zolotukhin I, et al. Production and purification of serotype 1, 2, and 5 recombinant adeno-associated viral vectors. *Methods*. 2002;28:158–167.
36. Kornfeld SF, Lynch-Godrei A, Bonin SR, Gibeault S, De Repentigny Y, Kothary R. Cytoskeletal linker protein dystonin is not critical to terminal oligodendrocyte differentiation or CNS myelination. *PLoS One*. 2016;11:e0149201.
37. Schneider CA, Rasband WS, Eliceiri KW. NIH Image to ImageJ: 25 years of image analysis. *Nat Methods*. 2012;9:671–675.
38. Tan E, Ding XQ, Saadi A, Agarwal N, Naash MI, Al-Ubaidi MR. Expression of cone-photoreceptor-specific antigens in a cell line derived from retinal tumors in transgenic mice. *Invest Ophthalmol Vis Sci*. 2004;45:764–768.
39. Riordan-Eva P, Sanders MD, Govan GG, Sweeney MG, Da Costa J, Harding AE. The clinical features of Leber's hereditary optic neuropathy defined by the presence of a pathogenic mitochondrial DNA mutation. *Brain*. 1995;118(Pt 2):319–337.
40. Nikoskelainen EK, Huoponen K, Juvonen V, Lamminen T, Nummelin K, Savontaus ML. Ophthalmologic findings in Leber hereditary optic neuropathy, with special reference to mtDNA mutations. *Ophthalmology*. 1996;103:504–514.
41. Shankar SP, Fingert JH, Carelli V, et al. Evidence for a novel x-linked modifier locus for Leber hereditary optic neuropathy. *Ophthalmic Genet*. 2008;29:17–24.
42. Zhang J, Zhao F, Fu Q, et al. Mitochondrial haplotypes may modulate the phenotypic manifestation of the LHON-associated m.14484T>C (MT-ND6) mutation in Chinese families. *Mitochondrion*. 2013;13:772–781.
43. Xie S, Zhang J, Sun J, et al. Mitochondrial haplogroup D4j specific variant m.11696G > a(MT-ND4) may increase the penetrance and expressivity of the LHON-associated m.11778G > a mutation in Chinese pedigrees. *Mitochondrial DNA A DNA Mapp Seq Anal*. 2017;28:434–441.
44. Kirkman MA, Yu-Wai-Man P, Korsten A, et al. Gene-environment interactions in Leber hereditary optic neuropathy. *Brain*. 2009;132:2317–2326.
45. Kotterman MA, Yin L, Strazzeri JM, Flannery JG, Merigan WH, Schaffer DV. Antibody neutralization poses a barrier to intravitreal adeno-associated viral vector gene delivery to non-human primates. *Gene Ther*. 2015;22:116–126.
46. Yao K, Qiu S, Wang YV, et al. Restoration of vision after de novo genesis of rod photoreceptors in mammalian retinas. *Nature*. 2018;560:484–488.
47. Li Q, Miller R, Han PY, et al. Intraocular route of AAV2 vector administration defines humoral immune response and therapeutic potential. *Mol Vis*. 2008;14:1760–1769.
48. Lin CS, Sharpley MS, Fan W, et al. Mouse mtDNA mutant model of Leber hereditary optic neuropathy. *Proc Natl Acad Sci USA*. 2012;109:20065–20070.
49. Yu H, Koilkonda RD, Chou TH, et al. Consequences of zygote injection and germline transfer of mutant human mitochondrial DNA in mice. *Proc Natl Acad Sci USA*. 2015;112:E5689–5698.
50. Evans MK, Sauer SJ, Nath S, Robinson TJ, Morse MA, Devi GR. X-linked inhibitor of apoptosis protein mediates tumor cell resistance to antibody-dependent cellular cytotoxicity. *Cell Death Dis*. 2016;7:e2073.
51. Koilkonda RD, Yu H, Chou TH, et al. Safety and effects of the vector for the Leber hereditary optic neuropathy gene therapy clinical trial. *JAMA Ophthalmol*. 2014;132:409–420.
52. Feuer WJ, Schiffman JC, Davis JL, et al. Gene therapy for Leber hereditary optic neuropathy: initial results. *Ophthalmology*. 2016;123:558–570.
53. Yu H, Porciatti V, Lewin A, Hauswirth W, Guy J. Longterm reversal of severe visual loss by mitochondrial gene transfer in a mouse model of Leber hereditary optic neuropathy. *Sci Rep*. 2018;8:5587.
54. Guy J, Feuer WJ, Davis JL, et al. Gene therapy for Leber hereditary optic neuropathy: low- and medium-dose visual results. *Ophthalmology*. 2017;124:1621–1634.
55. Vignal C, Uretsky S, Fitoussi S, et al. Safety of rAAV2/2-ND4 gene therapy for Leber hereditary optic neuropathy. *Ophthalmology*. 2018;125:945–947.
56. Bouquet C, Vignal Clermont C, Galy A, et al. Immune response and intraocular inflammation in patients with Leber hereditary optic neuropathy treated with intravitreal injection of recombinant adeno-associated virus 2 carrying the ND4 gene: a secondary analysis of a phase 1/2 clinical trial. *JAMA Ophthalmol*. 2019.
57. Cideciyan AV, Jacobson SG, Beltran WA, et al. Human retinal gene therapy for Leber congenital amaurosis shows advancing retinal degeneration despite enduring visual improvement. *Proc Natl Acad Sci USA*. 2013;110:E517–525.

Investigative Ophthalmology & Visual Science